journal homepage: www.elsevier.com/locate/jmatprotec

Texture and mechanical properties evolution of a deep drawing medium carbon steel during cold rolling and subsequent recrystallization

C. Herrera[a,*], *N.B. Lima*[b], *A. Ferreira Filho*[c], *R.L. Plaut*[d], *A.F. Padilha*[d]

[a] *Max-Planck-Institut für Eisenforschung GmbH, Department for Microstructure Physics and Metal Forming, Max-Planck-Straße 1, D-40237 Düsseldorf, Germany*
[b] *Instituto de Pesquisas Energéticas e Nucleares, CCTM, Av. Prof. Lineu Prestes, 2242, CEP 05508-900 S. Paulo, Brazil*
[c] *Brasmetal Waelzholz S.A., Rua Goiás, 501, CEP 09941-690 Diadema, Brazil*
[d] *Universidade de São Paulo, Departamento de Engenharia Metalúrgica e de Materiais, Av. Prof. Mello Moraes, 2463, CEP 05508-900 São Paulo, Brazil*

ARTICLE INFO

Article history:
Received 30 November 2007
Received in revised form
29 July 2008
Accepted 17 August 2008

Keywords:
Medium carbon steels
Texture
Mechanical properties
Deep drawing

ABSTRACT

Medium carbon steels are mostly used for simple applications; however, new applications have been developed for which good sheet metal formability is required. These types of steels have an inherent low formability. A medium-carbon hot-rolled SAE 1050 steel was selected for this study. It has been cold rolled with thickness reductions varying between 7 and 80%. The samples obtained were used to evaluate the strain hardening curve. For samples with a 50 and 80% thickness reduction, an annealing heat treatment was performed to achieve recrystallization. The material was characterized in the “as-received”, cold rolled and annealed conditions using several methods: optical metallography, X-ray diffraction (texture), Vickers hardness, and tensile testing. For large thickness reductions, the SAE 1050 steel presented low elongation, less than 2%, and yield strength (YS) and tensile strength (TS) around 1400 MPa. Texture in the “as-received” condition showed strong components on the $\{0\,0\,1\}$ plane, in the $\langle 1\,0\,0\rangle$, $\langle 2\,1\,0\rangle$ and $\langle 1\,\bar{1}\,0\rangle$ directions. After cold rolling, the texture did not present any significant changes for small thickness reductions, however. It changed completely for large ones, where gamma, $\langle 1\,1\,1\rangle$//ND, alpha, $\langle 1\,1\,0\rangle$//RD, and gamma prime, $\langle 2\,2\,3\rangle$//ND, fibres were strengthened. After annealing, the microstructure of the SAE 1050 steel was characterized by recrystallized ferrite and globular cementite. There was little change in the alpha fibre for the 50% reduction, whereas for the 80% reduction, its intensity increased. Both gamma and gamma prime fibres vanished upon annealing for 50 and 80% reductions alike.

1. Introduction

Carbon steels, particularly flat rolled sheets, are by far the most largely produced metallic materials around the world. However, most part of that production is employed for common applications, their processing technology and related mechanical properties have undergone continuous improvements and development. The most significant sector of the flat

* *Corresponding author*. Tel.: +49 211 6792429; fax: +49 211 6792333.
E-mail address: c.herrera@mpie.de (C. Herrera).
0924-0136/$ – see front matter © 2008 Elsevier B.V. All rights reserved.
doi:10.1016/j.jmatprotec.2008.08.007

Table 1 – Chemical composition (wt%) of the SAE 1050 studied steel

C	S	Mn	Si	P	Al	Mo	N	Ni
0.472	0.0044	0.705	0.1966	0.0155	0.0361	0.001	0.025	0.0106
Cr	Ti	Nb	V	Cu	Pb	Sn	B	W
0.0212	0.0023	0.0011	0.0003	0.017	0.0003	0.0008	0.0002	0.0022

rolled products is aimed at the stamping market, mainly the low carbon steels, employed in car manufacturing. Nevertheless, these steels have limitations in their applications when it comes to thermo-chemical treatments. Furthermore, due to their low carbon level, they are not appropriate for the heat treatments of quenching and tempering. Hence, their strength is low, limiting their use and consequently, calling for medium and high carbon steels.

Nowadays a large number of new applications for medium and high carbon steels have been developed which also require deep drawing. These steels present low workability and this condition becomes more critical as the carbon level is increased, when its workability drops substantially. A survey conducted by Storojeva et al. (2004a,b) in a medium carbon steels (0.36% C) has shown that the pearlite lamellar morphology leads to undesirable cold working mechanical properties in highly stressed components, while globular cementite morphology conduces to higher toughness, good cold workability and machinability.

Stampability mainly depends on the anisotropy and consequently, on texture. A body-centered cubic (BCC) material has an ideal texture for deep drawing when a large number of grains is oriented with its {1 1 1} plane parallel to the sheet plane. This type of texture is known as the γ-fibre ⟨1 1 1⟩//ND. The γ-fibre occurs along φ_1 at constant values of $\varphi_2 = 45^\circ$ and $\phi = 55^\circ$. Two excellent reviews on cold rolling and annealing textures and the relation with the drawability in low carbon steels have been published by Hutchinson (1984) and Ray et al. (1994). In addition, there has been a recent overview by Humphreys and Hatherly (2004) on texture in BCC materials. The β-fibre, which is a skeleton line, also has influence on the deep drawing. The skeleton line is defined as a line connecting the points of maximum intensity in the φ_1 section, thus having variable φ_2 and ϕ coordinates. Daniel and Jonas (1990) and Daniel et al. (1993) studied anisotropy in deep-drawing steels. These works concluded that deep-drawing steels develop a

Fig. 1 – Microstructure of SAE 1050 steel-"as received" condition.

strong γ-fibre and the skeleton line deviates somewhat from the γ-fibre passing through the {5 5 4}⟨2 2 5⟩ orientation. The spread about the normal direction (ND) varies with the steel type and φ_1. The greater the dispersion about the skeleton line, the lower the *r*-values and the lower the material drawability.

The texture of medium and high carbon steels in different conditions such as hot rolled, cold rolled or annealed has not been investigated in depth. Storojeva et al. (2004a,b) conducted research on the texture evolution and the microstructure of a warm rolled medium carbon steel (0.36% C–0.53% Mn–0.22%

Table 2 – Mechanical properties of the SAE 1050 steel-"as received" condition

YS (N/mm^2)	TS (N/mm^2)	El80 (%)	Hardness (HV)
665	833	7.2	227

YS, Yield strength; TS, tensile strength; El(80), elongation in 80 mm.

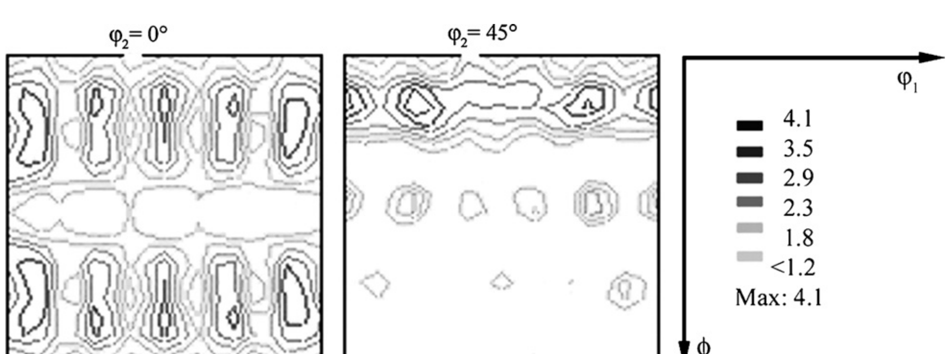

Fig. 2 – ODF of the SAE 1050 steel in the "as received" condition.

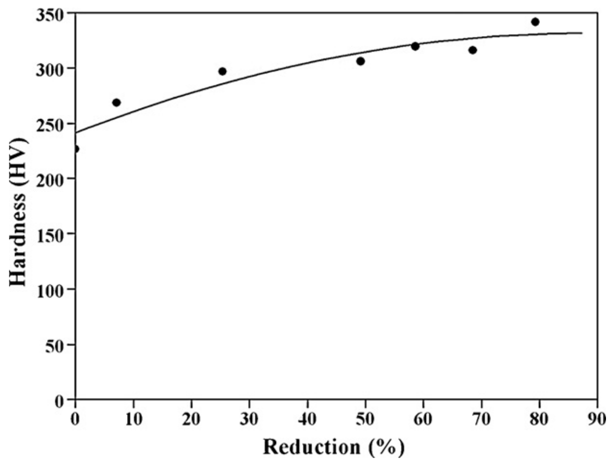

Fig. 3 – Strain hardening curve.

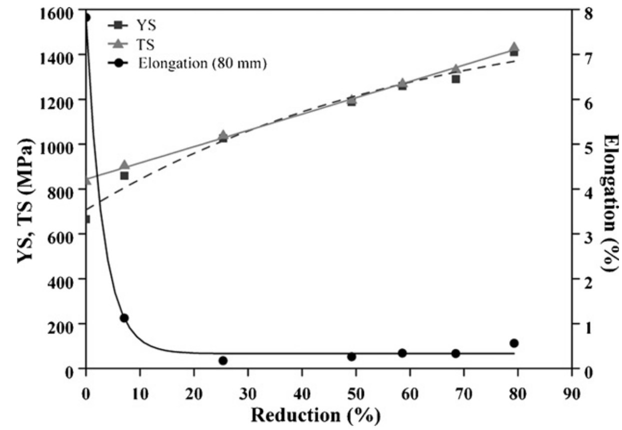

Fig. 4 – Mechanical properties as a function of cold reduction.

Si). They concluded that the texture does not change for different rolling and coiling temperatures, texture being characterized by the γ- and α-fibres with a maximum of the {1 1 2}⟨1 1 0⟩ component. Walenteck et al. (2005) studied the texture evolution in high carbon steel (0.79% C–0.9% Mn–0.26% Si) which underwent 74% reduction in thickness. They concluded that the resulting deformation texture was that typical of the BCC cold rolled materials, characterized by the γ- and α-fibres, but with a much lower intensity when compared to those of a low carbon steel.

Some researchers, Fujita et al. (2005), Ray et al. (1994) and Walenteck et al. (2005), have carried out the study of the effect of different variables, such as chemical composition and processing parameters on the deformation texture. They conclude that the deformation texture development in low and high carbon steels is affected by the difference in the initial texture as well as by the presence and distribution of a second phase such as cementite in higher carbon steels. Deformation texture was simulated for both steels by Walenteck et al. (2005). Their results suggest that the grain interaction has greater influence on the deformation texture than the effect caused by the presence of a second phase, i.e. the cementite lamella.

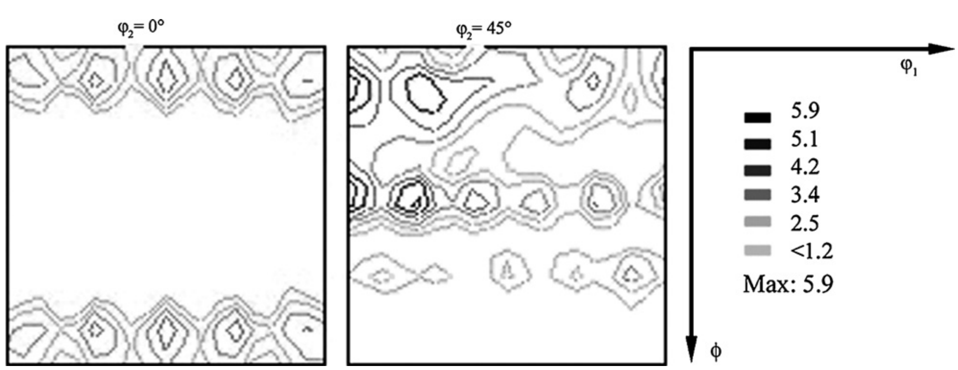

Fig. 5 – ODF of the SAE 1050 steel with a 50% thickness reduction.

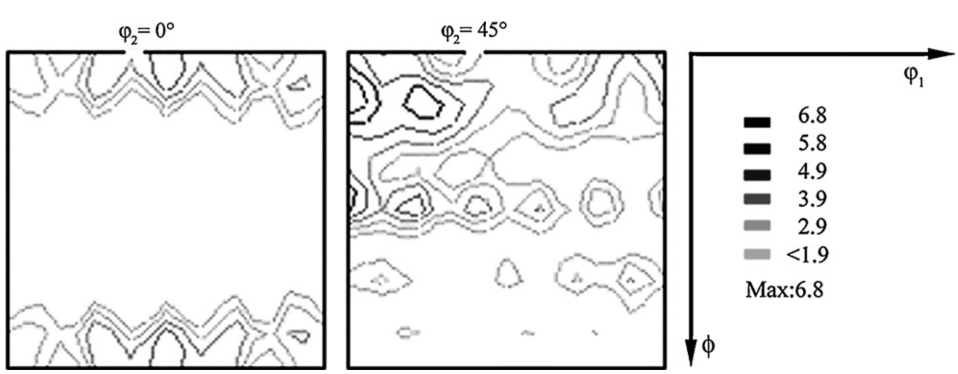

Fig. 6 – ODF of the SAE 1050 steel with a 70% thickness reduction.

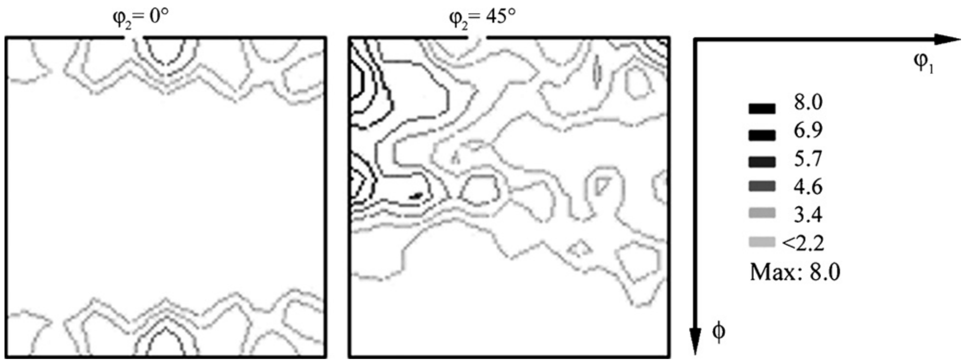

Fig. 7 – ODF of the SAE 1050 steel with 80% thickness reduction.

The objective of the present work is to study the texture and the mechanical properties of medium carbon steel in the different processing stages, aiming at understanding its behavior during stamping.

2. Experimental procedure

A medium-carbon steel SAE 1050 was selected, hot rolled to the nominal thickness of 2.65 mm (produced by CST, Brazil). Table 1 presents the chemical composition of the studied material.

The steel was cold rolled with thickness reductions ranging from 7 to 80% aiming at the evaluation of the cold work hardening curve. The cold rolling operation was carried out on a reversing four-high industrial mill at Brasmetal Waelzholz.

Heat treatments were performed on the 50 and 80% cold rolled samples at 700 °C for 13 h under 100% H_2 atmosphere using an industrial furnace, in order to promote full recrystallization.

For the material characterization in distinct conditions (i.e. "as-received", cold rolled and annealed) different techniques such as optical microscopy, X-ray diffraction (texture), Vickers hardness and tensile testing were employed.

Texture evolution in the three different conditions was evaluated by X-ray diffraction technique using a Rigaku horizontal texture goniometer. Measurements were carried out with Mo Kα1 (λ = 0.07093 nm) radiation using the back reflection technique as described by Schulz (1949). Four incomplete pole figures {1 1 0}, {2 0 0}, {2 1 1} and {3 1 0} ($5° \leq \alpha \leq 70°$) were measured. From these pole figures, ODF (Orientation Distribution Function) were calculated by the series expansion method (l_{max} = 22) using generalized spherical harmonics as proposed by Bunge (1982). All analysis was performed on the sheet sample surface.

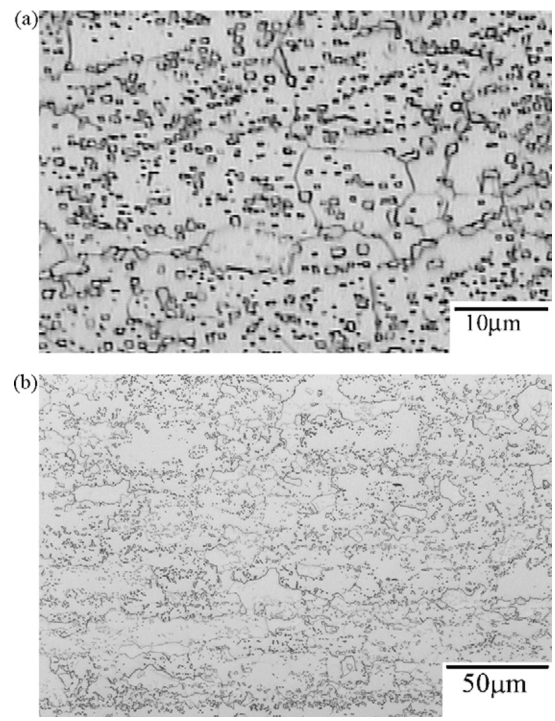

Fig. 8 – SAE 1050 steel cold worked (a) 50% and (b) 80%, annealed.

Tensile tests were carried out using a Zwick model-1475 universal testing machine equipped with hydraulic chucks and extensometer. Sample dimensions were machined

Table 3 – Mechanical properties of the SAE 1050 cold worked and annealed

Red. (%)	YS (N/mm^2)	TS (N/mm^2)	El80 (%)	n	r_m	Δr	Hardness (HV)	E.I. (mm)
50	333	491	24.4	0.19	0.85	0.22	144	11.8
80	304	471	28.6	0.18	1.07	−1.28	142	9.0

YS, Yield strength; TS, tensile strength; El(80), elongation in 80 mm; n, strain hardening coefficient; r_m, normal anisotropy index; Δr, planar anisotropy index; E.I., Erichsen index.

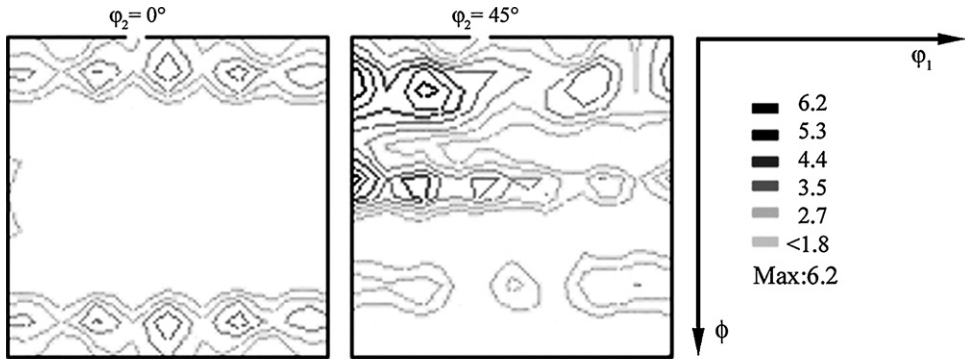

Fig. 9 – ODF of the 1050 steel for 50% cold reduction, annealed.

according to the ASTM standard. From the tensile testing the values of yield strength (YS), tensile strength (TS), total elongation (strain to fracture), strain hardening coefficient or exponent (n), normal anisotropy index (r_m) and planar anisotropy index (Δr) were evaluated.

3. Results and discussion

The SAE 1050 steel in the "as-received" condition presented a microstructure composed of pearlite and ferrite (Fig. 1) and a hardness of 226 HV. Table 2 shows the mechanical properties in the "as-received" condition. Texture was characterized by the strong components in the {0 0 1} planes, in the ⟨1 0 0⟩, ⟨2 1 0⟩ and ⟨1 $\bar{1}$ 0⟩ directions, TR = 4.1, where TR stands for Times Random. The γ- and α-fibres were absent (Fig. 2).

Strain hardening was studied by Vickers hardness measurements performed in a section normal to the rolling direction. The SAE 1050 steel showed very small strain hardening, i.e. small hardness variation with increasing strain level (Fig. 3). For larger strains (over 30%) hardness tends towards saturation.

Fig. 4 shows the changes in mechanical properties, that is yield and tensile strength as well as elongation with cold reduction. The difference between the yield and tensile strength decreases with thickness reduction that is the load required for the material to rupture is very close to the load required for yielding. For higher levels of strain hardening, the SAE 1050 steel presents an elongation lower than 2%, and yield and tensile strength in the order of 1400 MPa. In the strain hardened condition, the steel shows low ductility, i.e. it takes higher loads but lower elongation, mainly due to its ferrite/pearlite microstructure. Cementite hinders the dislocation mobility; hence, higher stresses are required in order to move the dislocations.

Figs. 5–7 illustrate the ODFs for the SAE 1050 steel for 3 levels of reduction in thickness: 50, 70 and 80%. For cold reductions higher than 50%, texture changed completely from the "as-received" condition. The deformation texture was characterized by the γ′-fibre, ⟨2 2 3⟩//ND, with the {2 2 3}⟨1 1 0⟩, {2 2 3}⟨4 7 2⟩ and {2 2 3}⟨1 4 2⟩ as the most intense components, TR = 5.9, the ⟨1 0 0⟩//ND fibre with the {0 0 1}⟨1 1 0⟩ and {0 0 1}⟨1 2 0⟩ components and the α-fibre, ⟨1 1 0⟩//RD, weak and heterogeneous. The γ′-fibre is that characteristic of the cold rolled low carbon steels; it lies parallel to the γ-fibre and is situated at $\Phi = 43.3^\circ$ in the $\varphi_2 = 45^\circ$ section. This fibre is a variant of the γ-fibre, i.e. a rotation around the ⟨1 1 1⟩ axis, that has early described by Daniel et al. (1993) and Inagaki (1994).

Further thickness reduction up to 70% led to a weakening in the ⟨1 0 0⟩//ND and γ′-fibres. In contrast, the (0 0 1)[1 2 0], (0 0 1)[1 1 0] and (2 2 3)[1 $\bar{1}$ 0] components became more intense, TR = 6.8, the two last ones belonging to the α-fibre. With 80% thickness reduction, the α-fibre continued to strengthen with the more intense {0 0 1}⟨1 1 0⟩ and {2 2 3}⟨1 1 0⟩ components, TR = 8. The γ-fibre, which did not appear for lower reductions, started to appear with some dispersion from the (1 1 0)[1 $\bar{1}$ 0] to the (5 5 4)[2 2 $\bar{5}$] components and the γ′-fibre decreased in intensity.

Many researchers, Humphreys and Hatherly (2004), Hutchinson (1984), Raabe and Lücke (1994) and Inagaki (1994),

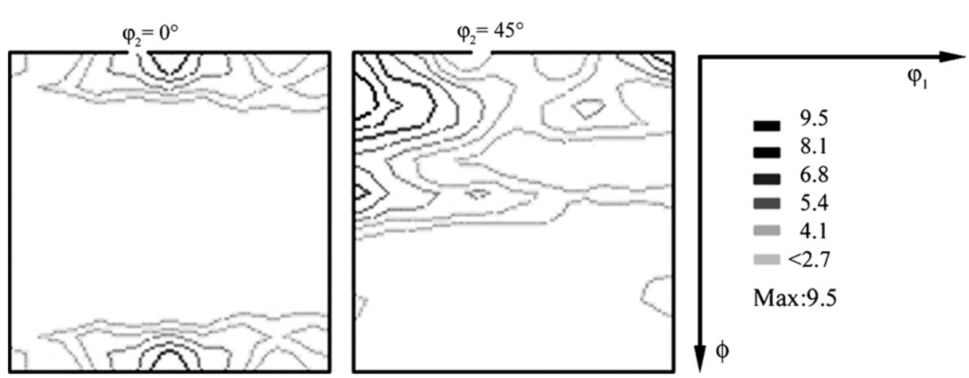

Fig. 10 – ODF of the SAE 1050 steel for 80% cold reduction, annealed.

have pointed out that the main deformation textures observed in BCC are the α-fibre, ⟨1 1 0⟩//RD, which includes the components {0 0 1}⟨1 1 0⟩, {2 1 1}⟨1 1 0⟩ and {1 1 1}⟨1 1 0⟩, and γ-fibre, ⟨1 1 1⟩//ND. It should be stressed that this deformation texture has been previously reported by Fujita et al. (2005), Fukui and Okamoto (1990) and Walenteck et al. (2005) for medium and high carbon steels. The results confirm that the cold rolled texture of the SAE 1050 steel is typical of cold rolled BCC materials.

Fig. 8 presents the microstructure of the SAE 1050 steel with 50 and 80% thickness reduction and annealed, with its typical microstructure composed of a ferritic matrix and globular cementite. Table 3 shows the mechanical properties of the annealed SAE 1050 steel for both reductions. The yield and tensile strength presented a significant decrease after annealing, whereas elongation increased if compared to the "as-received" condition.

For the annealed 80% cold-worked sample the yield and tensile strengths as well as the Erichsen index were lower, whereas the elongation was larger than the one observed for the annealed 50% cold-worked sample. Although the r_m value has increased with the amount of cold reduction, the large value of Δr is detrimental to the drawabilty of the steel, since the main goal in deep drawing is to maximize r_m and to minimize Δr ($\Delta r = 0$).

Figs. 9 and 10 present the ODFs for the annealed and cold-worked 50 and 80% thickness-reduced steels, respectively. The SAE 1050 annealed 50% cold-worked steel presented more intense (0 0 1)[1 $\bar{1}$ 0] and (2 2 3)[1 $\bar{1}$ 0] components, TR = 6.2. The last one belongs to the γ′-fibre, ⟨2 2 3⟩//ND, which presented lower intensity, similar to the semi-α-fibre ⟨0 1 1⟩//RD. The SAE 1050 annealed 80% cold-rolled steel exhibited a semi-α-fibre, ⟨0 1 1⟩//RD, with a (2 2 3)[1 $\bar{1}$ 0] component and a more intense one near (0 0 1)[1 $\bar{1}$ 0] component, TR = 9.5. The γ-fibre did not appear in these samples.

Fig. 11 summarizes the texture evolution of the steel for different conditions, e.g. cold worked and annealed, along the γ, γ′ and α-fibres, presented in the steel. The γ-fibre (Fig. 11a) became intensified with deformation, even though its intensity was not high in comparison to the α-fibre. If this result is compared to the one obtained for the high carbon by Walenteck et al. (2005), one observes that although the γ-fibre in the high carbon steel is more homogeneous and its intensity is lower (close to 5), i.e. during the rolling of steels with a second phase, the deformation textures are weaker. After annealing, the γ-fibre vanished.

The γ′-fibre (Fig. 11b) did not present any significant variation for the smaller reductions, whereas for larger ones, e.g. 80% thickness reduction, its intensity drops. After annealing, the γ′-fibre for the 50% cold worked steel did not show major changes, yet for 80% cold reduction, it vanished completely.

The α-fibre (Fig. 11c) became more intense with the reduction increase, and the {2 2 3}⟨1 1 0⟩ and the close to {0 0 1}⟨1 1 0⟩ components were stronger. The {1 1 1}⟨1 1 0⟩ component that did not show up for lighter reductions, weakly appeared only after annealing of the 80% thickness-reduced specimen, the α-fibre showed some strengthening between the {0 0 1} and {1 1 2} planes.

Annealing of the SAE 1050 steel after different reductions did not significantly change the deformation texture. This behaviour has been reported by Fujita et al. (2005) and Fukui and Okamoto (1990) in high carbon steels. They have shown that the volume fraction, morphology and distribution of the second phase have a big influence on the recrystallization process. Fukui and Okamoto (1990) investigated the effect of graphite and cementite on mechanical properties of cold rolled high carbon steels. They found that, after recrystallization, the {1 1 1} and {1 0 0} textures formed by cold rolling were maintained in the ferrite-cementite steel, while a random texture was formed in ferrite-graphite steel.

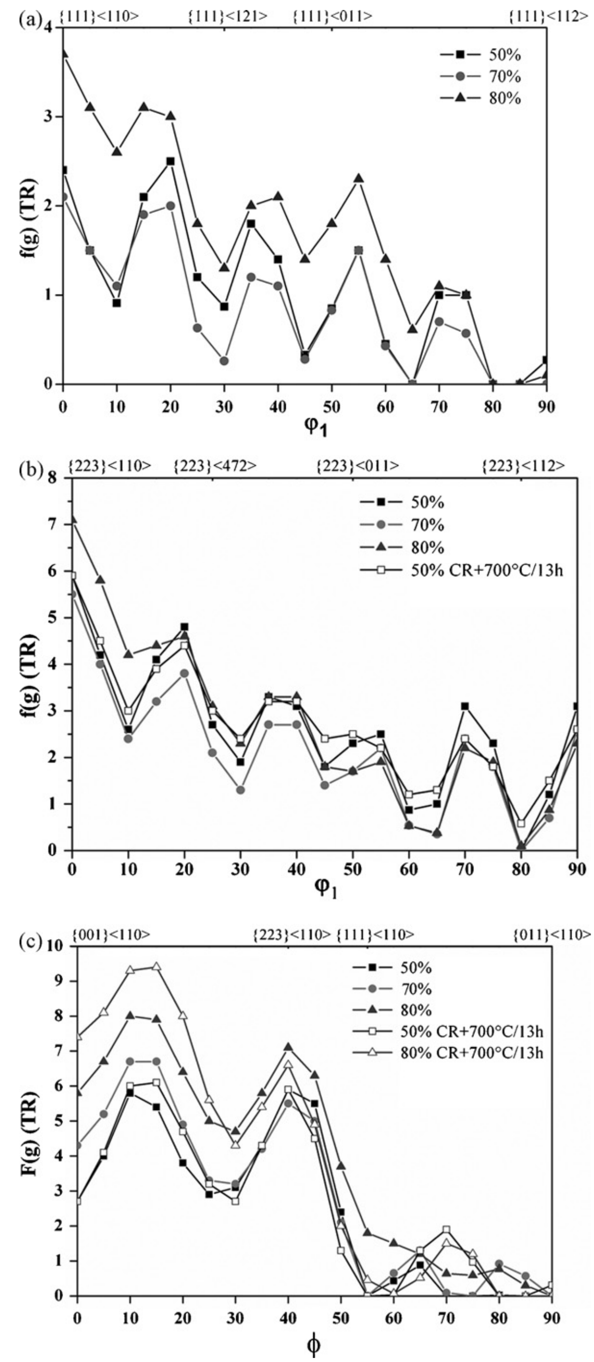

Fig. 11 – Evolution of the (a) γ-fibre, (b) γ′-fibre and (c) α-fibre of the annealed SAE 1050 steel for different reductions.

The results show that, for larger reductions, annealing texture increased the intensity of the α-fibre, whereas the γ- and γ′-fibres vanished. The high dislocation density and its favourable distribution in the steel leads to the development of α-fibre texture components during recrystallization. A deformation close to 50% produced a better texture for deep drawing than higher deformations due to the presence of γ′-fibre that is close to the γ-fibre. This result is consistent with those of Fujita et al. (2005), who showed that the Δr had its maximum value at 50% cold-rolling reduction with a secondary annealing temperature of 680 °C.

4. Conclusions

The SAE 1050 steel in the “as received” condition presented a microstructure containing pearlite and ferrite, with a weak texture in which the α- and γ-fibres were absent.

Strain hardening of the SAE 1050 steel was very low. For high strain levels, it showed elongation lower than 2%, and yield and tensile strengths in the range of 1400 MPa. The textures observed were those typical of cold worked BCC metals.

The annealing texture did not show significant changes if compared to the deformation texture. For higher strains, the annealing texture presented some increase in the α-fibre, whereas the γ- and γ′-fibres vanished. A deformation close to 50% produced a better texture for drawing because the γ′-fibre is close to the γ-fibre.

After annealing, the yield and tensile strength decreased. In contrast the elongation increased with prior deformation. The r_m and Δr values increased with deformation, the increase in the value of Δr being a drawback for the drawability of the steel.

Acknowledgements

The authors are indebted to Brasmetal Waelzholz for its support during the experimental part and for the production of the samples. The CNPq (Brazil) is acknowledged for the financial support of an industrial post-doctoral project (Process no. 308839/2005-6).

REFERENCES

Bunge, H.J., 1982. Texture Analysis in Materials Science—Mathematical Methods. Buttherworth, London.
Daniel, D., Jonas, J.J., 1990. Measurement and predicting of plastic anisotropy in deep-drawing steels. Metall. Trans. A 41, 331–343.
Daniel, D., Savoie, J., Jonas, J.J., 1993. Texture induced by tension and deep drawing in low carbon and extra low carbon steel sheets. Acta Metall. Mater. 41, 1907–1920.
Fujita, T., Nakamura, N., Urabe, T., Okuda, K., Hosoya, Y., 2005. Effect of cold-rolling reductions on planar anisotropy of r-value in cold-rolled high carbon steel sheets. J. Jpn. Inst. Met. 69, 421–428.
Fukui, K., Okamoto, A., 1990. Effect of graphite, cementite on mechanical properties of cold rolled. J. Iron Steel Inst. Jpn. 76, 1349–1355.
Humphreys, F.J., Hatherly, M., 2004. Recrystallization and Related Annealing Phenomena, second ed. Elsevier, Oxford.
Hutchinson, W.B., 1984. Development and control of annealing textures in low-carbon steels. Int. Met. Rev. 29, 25–42.
Inagaki, H., 1994. Fundamental aspects of texture formation in low carbon steel. ISIJ Int. 34, 313–321.
Raabe, D., Lücke, K., 1994. Rolling and annealing texture of BCC metals. Mater. Sci. Forum 157–162, 597–610.
Ray, R.K., Jonas, J.J., Hook, R.E., 1994. Cold rolling and annealing textures in low carbon and extra low carbon steels. Int. Mat. Rev. 39, 129–172.
Schulz, L.G., 1949. Determination of preferred orientation in flat transmission samples using a Geiger counter X-ray spectrometer. J. Appl. Phys. 20, 1030–1033.
Storojeva, L., Ponge, D., Kaspar, R., Raabe, D., 2004a. Development of microstructure and texture of medium carbon steel during heavy warm deformation. Acta Mater. 52, 2209–2220.
Storojeva, L., Ponge, D., Raabe, D., Kaspar, R., 2004b. On the influence of heavy warm reduction on the microstructure and mechanical properties of a medium-carbon ferritic-pearlitic steel. Z. Metallkd. 95, 1108–1114.
Walenteck, A., Hu, X., Seefeldt, M., Van Houtte, P., 2005. Texture evolution cold rolling of low and high carbon steel. Measurement and simulation. Mater. Sci. Forum 495–497, 369–374.